



Geant4 Medical Physics applications at University of Naples Federico II



sarno@na.infn.it



“Siehe Neapel und Stirb” J. W. Goethe



“Siehe Neapel und Stirb” J. W. Goethe



“Siehe Neapel und Stirb” J. W. Goethe



“Siehe Neapel und Stirb” J. W. Goethe



The team at Medical Physics Research Lab today



Paolo Russo
Professor
Univ Naples Federico II
INFN Napoli



Giovanni Mettivier, Phd
Associate professor
Univ Naples Federico II
INFN Napoli



Antonio Sarno, Phd, Ing
Research Associate
Univ Naples Federico II
INFN Napoli



Daniele Esposito, Phd, Ing
Post-doc researcher
INFN Napoli



Laura Cerbone
PhD Student
Scuola Superiore Meridionale, Napoli
INFN Napoli



Physics Modeling

- ❑ Standard-EGS4 does not create/transport fluorescent photons
- ❑ Substitute sampling routine SUBROUTINE PHOTO allows for generation of K_{α_1} and K_{β_1} fluorescent photons.
 - Originally developed by Nelson and Jenkins in 1985.
 - Now used as standard in UNIX and PC distributions.
 - Switch (IEDGFL) turns on fluorescence by geometry region.
 - Requires auxiliary subroutine EDGSET (extended by K. Weaver (UCSF) to include all 100 elements).

- Del Guerra et al. (1991)^[11] have developed K and L-edge sampling scheme for compounds.

DISCLAIMER

This report was prepared in an account of work sponsored by an agency of the United States Government. Neither the United States Government nor any agency thereof, nor any of its employees, makes any warranty, express or implied, or assumes any legal liability or responsibility for the accuracy, completeness, or usefulness of any information, apparatus, product, or process disclosed, or represents that its use would not infringe privately owned rights. Reference herein to any specific commercial product, process, or service by trade name, trademark, manufacturer, or otherwise does not necessarily constitute or imply its endorsement, recommendation, or favoring by the United States Government or any agency thereof. The views and opinions of authors expressed herein do not necessarily state or reflect those of the Government.

EGS4 in '94

A Decade of Enhancements*

W. R. NELSON
Radiation Physics Department
Stanford Linear Accelerator Center
Stanford University, Stanford, California 94309, USA

A. F. BIELAJEW AND D. W. O. ROGERS
Institute for National Measurement Standards
National Research Council of Canada
Ottawa, K1A 0R6, Canada

H. HIRAYAMA
National Laboratory for High Energy Physics
1-1 Oho, Tsukuba-shi, Ibaraki-ken, 305, Japan

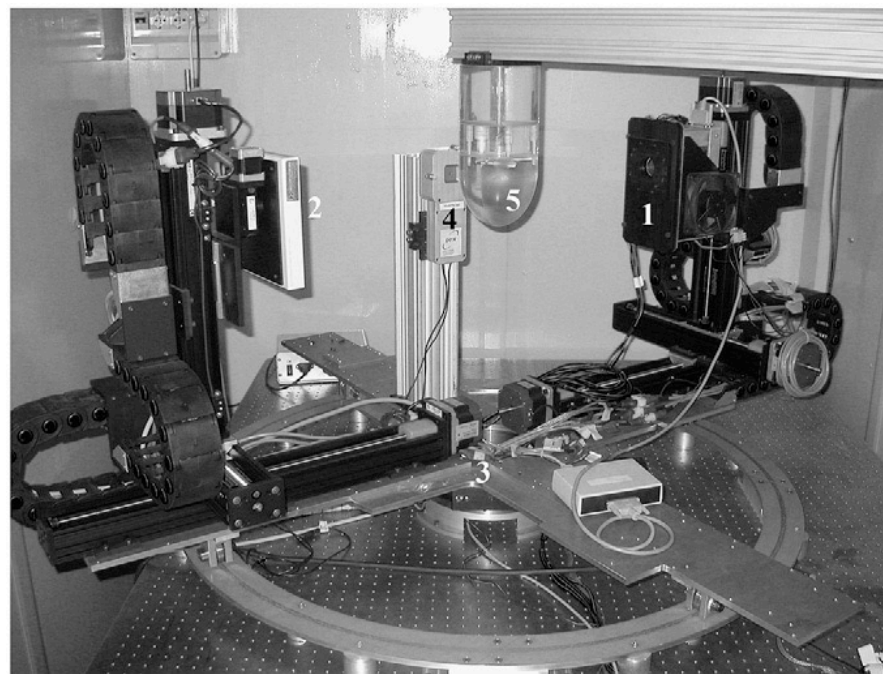
Presented at the World Congress on Medical Physics and Biomedical Engineering
21-26 August 1994, Rio de Janeiro, Brazil

1994: EGS4 Course held in Capri (first time outside North America)

Recent genesis: 3D breast CT - first prototype in Europe in 2008



Prof. John Boone inaugurates the new BCT prototype in Sep 2009



8 degrees of freedom step-motor drives
Microfocus X-ray tube (80 kV, 0.5 mA)
Breast dedicated CT and SPECT imaging

Geant4 for scatter correction in breast CT

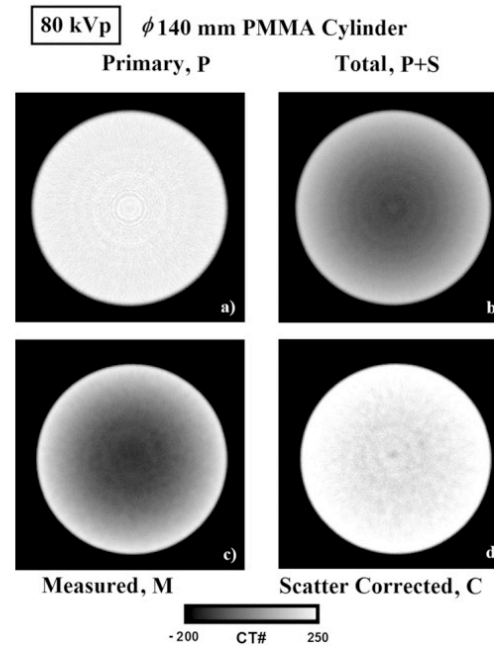
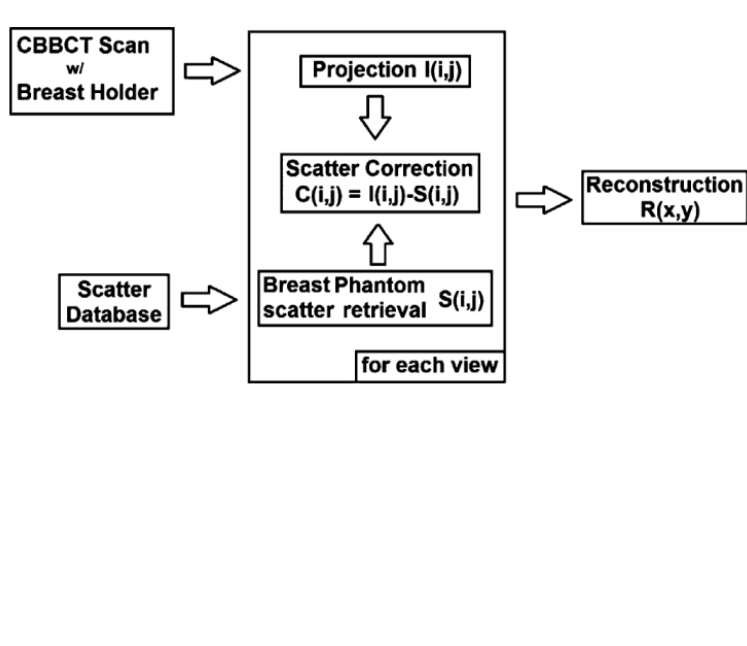


Fig. 8. Simulated primary (a), simulated total (b), measured (c) and scatter-corrected (d) reconstructed axial slices (at 80 kVp) of the 140-mm PMMA cylindrical phantom.

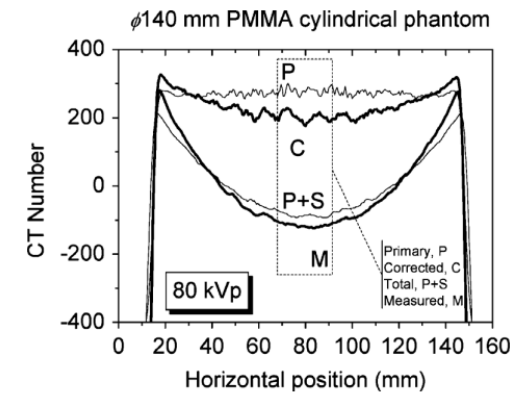


Fig. 9. Line profiles along the diameter of a 140-mm diameter PMMA cylinder on a reconstructed axial slice, at 80 kVp, obtained from simulated primary components only, from simulated total signal (primary plus scatter), from measurements and from measured data corrected for scatter.

Mettivier, G., Russo, P., Lanconelli, N., & Meo, S. L. (2010). Evaluation of scattering in cone-beam breast computed tomography: a Monte Carlo and experimental phantom study. *IEEE Transactions on Nuclear Science*, 57(5), 2510-2517.

Mettivier G, Lanconelli N, Meo SL & Russo, P. (2012). Scatter correction in cone-beam breast computed tomography: simulations and experiments. *IEEE Transactions on Nuclear Science*, 59(5), 2008-2019.

Geant4 for dose distribution assessment in x-ray breast imaging

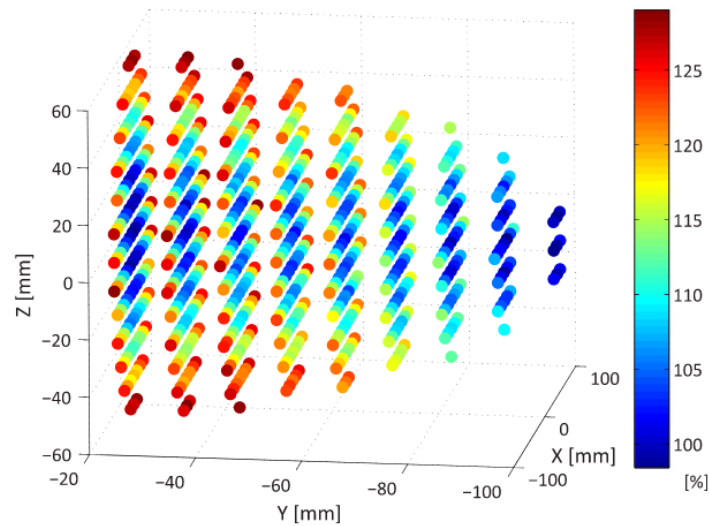


Figure 4 3D dose distribution of the PMMA breast phantom irradiated with the 80 kVp beam. The 3D position (x,y,z) of the different voxels is represented along the 3 coordinate axes, whereas their dose values are shown with a color map. Data are normalized to the minimum value registered. The y-axis is directed along the scanner rotation axis, with chest wall at left and nipple at right.

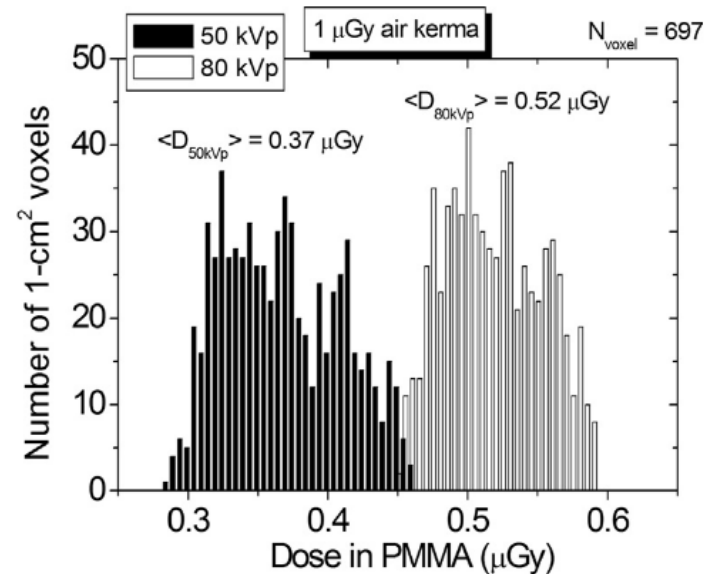
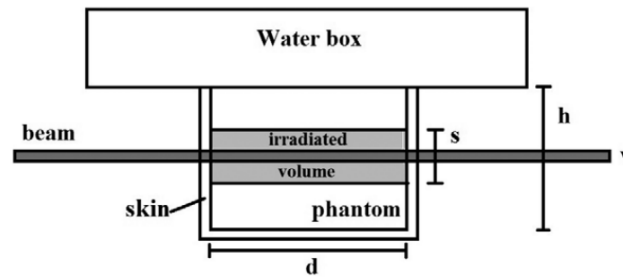
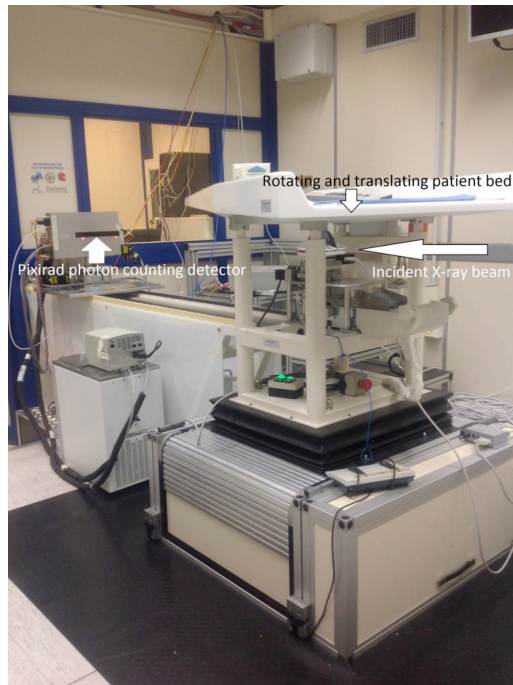


Figure 6 Histogram of the dose in PMMA breast phantom for two different beams: 50 kVp (black), and 80 kVp (white). The free-in-air air kerma at isocenter was fixed at 1 μ Gy.

Lanconelli N, Mettivier G, Meo SL & Russo, P. (2013). Investigation of the dose distribution for a cone beam CT system dedicated to breast imaging. *Physica Medica*, 29(4), 379-387.

New technologies requires new models: partial breast irradiation with a synchrotron radiation beam

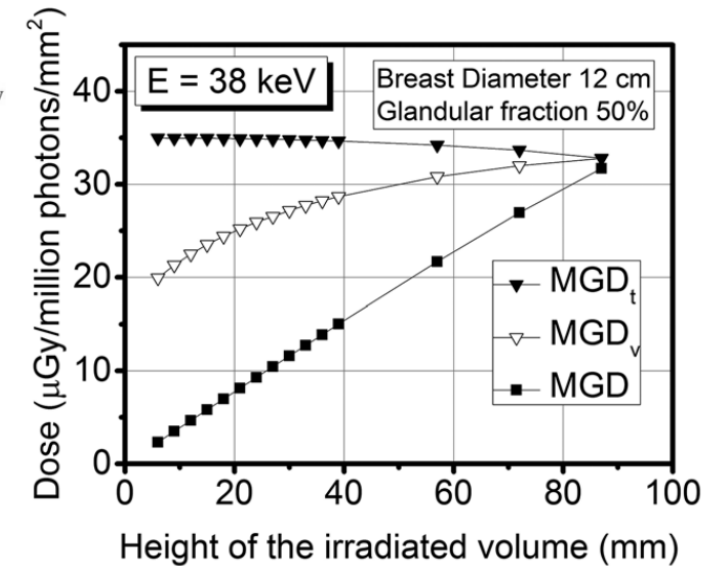
SYRMA-CT/SYRMA3D INFN national project



$$MGD = \frac{E_M}{M}$$

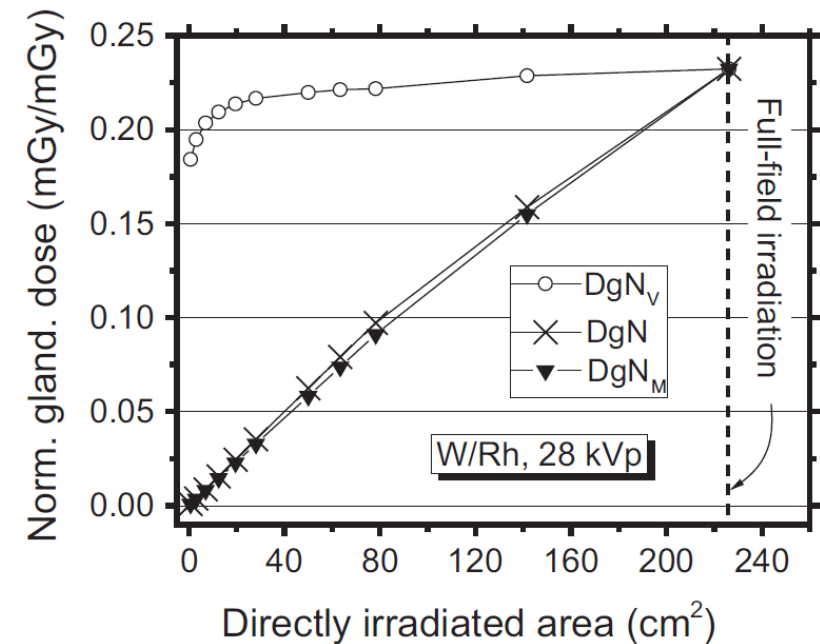
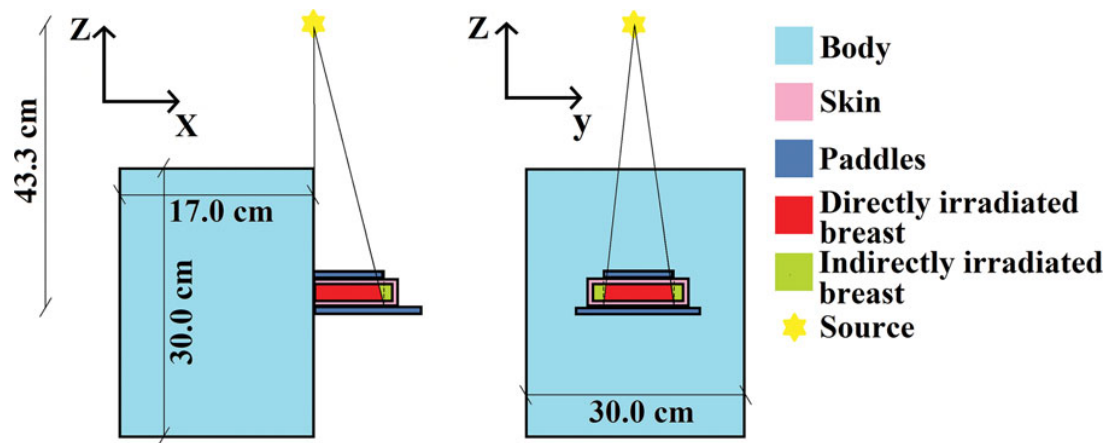
$$MGD_t = \frac{E_M}{m}$$

$$MGD_V = \frac{E_m}{m}$$



Mettivier, G., Fedon, C., Di Lillo, F., Longo, R., Sarno, A., Tromba, G., & Russo, P. (2015). Glandular dose in breast computed tomography with synchrotron radiation. *Physics in Medicine & Biology*, 61(2), 569.

The case of spot mammography dosimetry: a European collaboration



Sarno, A., Dance, D. R., Van Engen, R. E., Young, K. C., Russo, P., Di Lillo, F., ... & Sechopoulos, I. (2017). A Monte Carlo model for mean glandular dose evaluation in spot compression mammography. *Medical physics*, 44(7), 3848-3860.

Adoption of a new skin model for mammography dosimetry

Breast CT for finer skin model: 1.45 mm thick instead of the supposed 4-5 mm

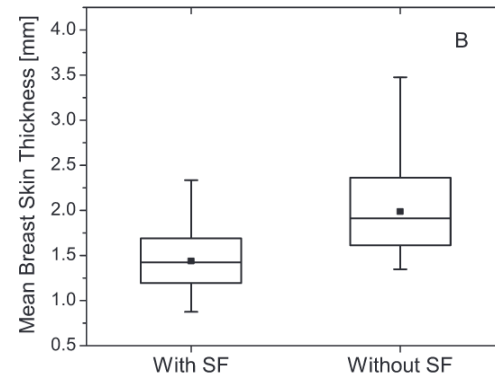
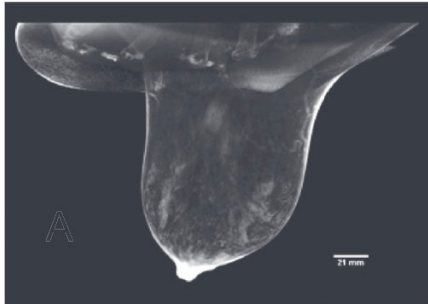
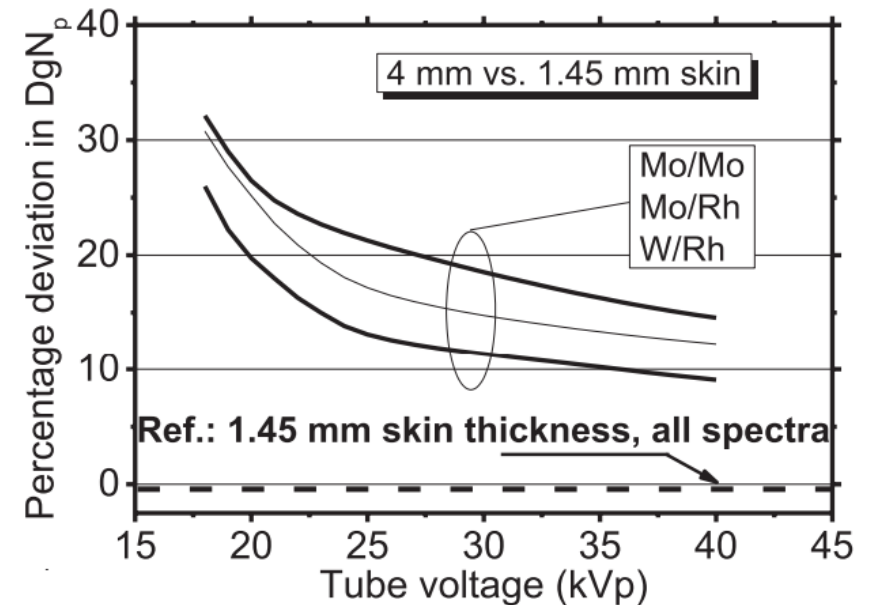


FIG. 1. Histogram (a) and box-plot (b) of the mean (location-averaged) breast skin thickness estimated with and without surface fitting (SF) the segmented skin layer. In the box-plot (b), the symbol within the box represents the mean, the horizontal line within the box represents the median, the box boundaries represent the ± 1 SD, and the whiskers represent the minimum and maximum. Wilcoxon signed ranks test indicated that there was a significant difference at the 0.05 level between the two methods ($p = 3.2 \times 10^{-24}$).

Shi L et al. "Skin thickness measurements using high-resolution flat-panel cone-beam dedicated breast CT." *Med Phys* 40.3 (2013): 031913.

Huang S-Y et al. "The effect of skin thickness determined using breast CT on mammographic dosimetry." *Med Phys* 35.4 (2008): 1199-1206.



Sarno, A., Mettivier, G., Di Lillo, F., & Russo, P. (2016). A Monte Carlo study of monoenergetic and polyenergetic normalized glandular dose (DgN) coefficients in mammography. *Physics in Medicine & Biology*, 62(1), 306.

Recalculation of dose conversion coefficients in DM and DBT

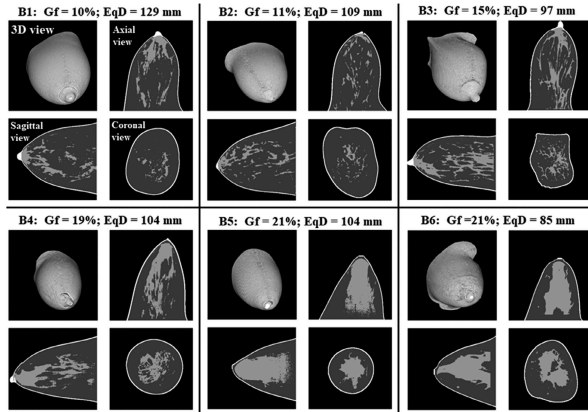
	A	B	C	D
1	<i>I_DgNdbt v.1.0</i>			
2				
3	DBT system	Siemens_Mammomat_Inspiration		
4				
5	Breast thickness (20 - 90 mm)	88.0	Tube Voltage (kV)	32
6				
7	HVL (mm Al)	0.522	Glandular fraction by mass (%) (1-100)	40.0
8		Beam HVL Type the 1st HVL in mm Al		
9	Interpolated DgN (mGy/mGy air kerma) CC view	0.160	Input validated	
10				
11	Color legend:	Input data from the user	Result	

Sarno A et al. "Monte Carlo calculation of monoenergetic and polyenergetic DgN coefficients for mean glandular dose estimates in mammography using a homogeneous breast model." *Phys Med Biol* 64.12 (2019): 125012.

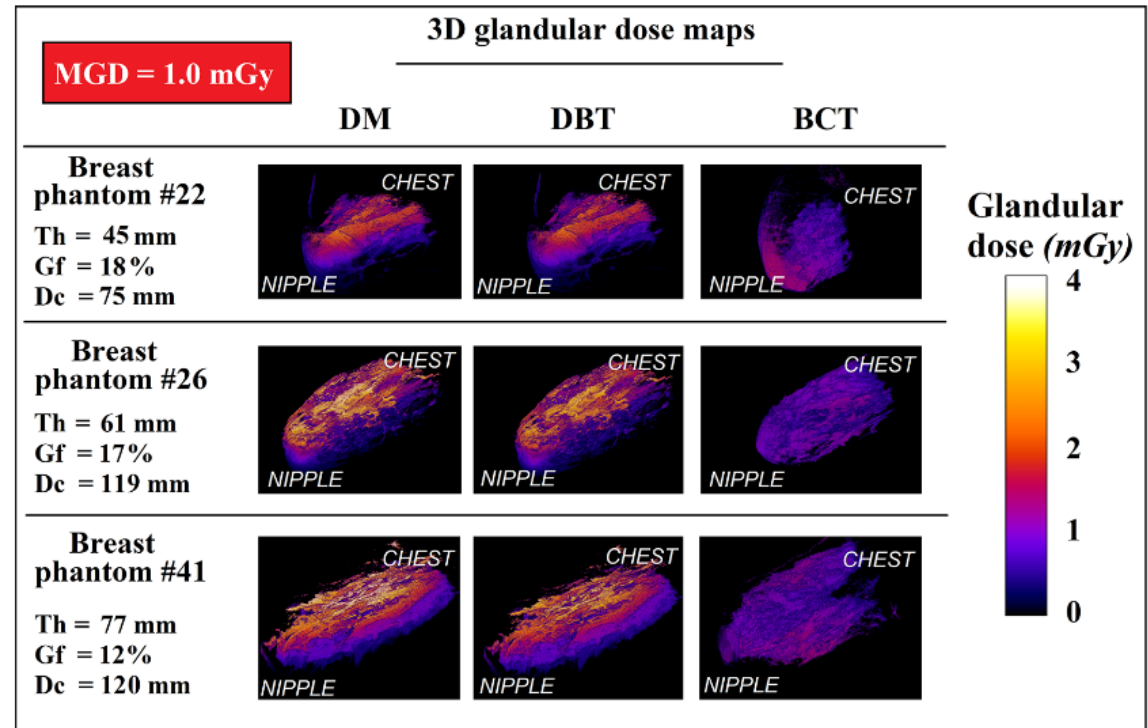
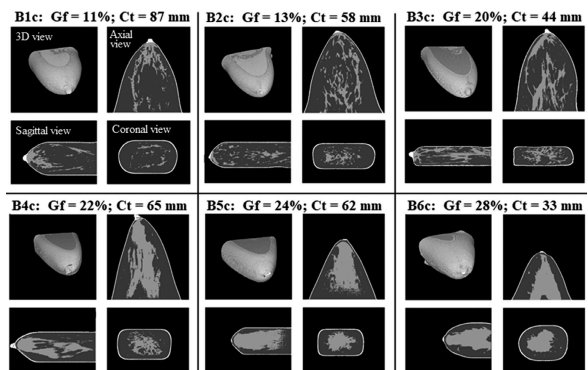
Sarno A et al. "Normalized glandular dose coefficients for digital breast tomosynthesis systems with a homogeneous breast model." *Phys Med Biol* 66.6 (2021): 065024.

Homogeneous vs. non-homogeneous models in x-ray breast imaging

Patient-derived uncompressed digital breast phantoms



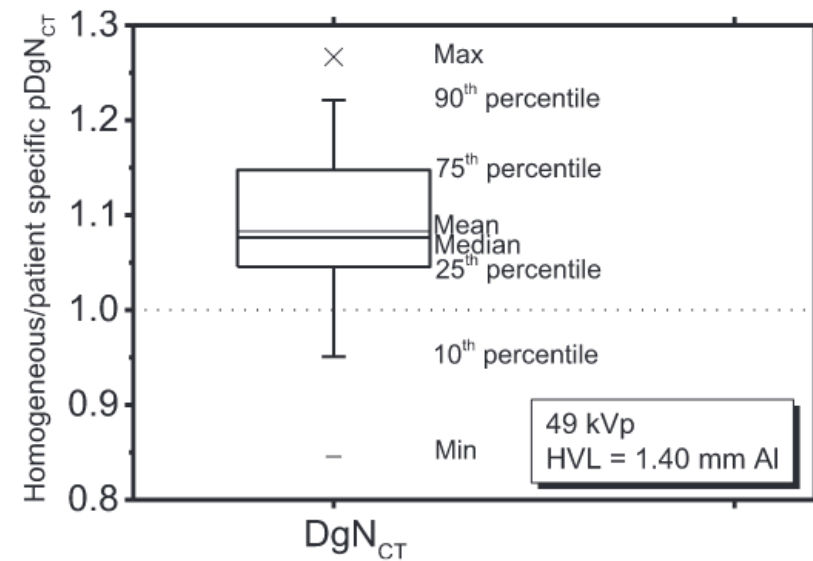
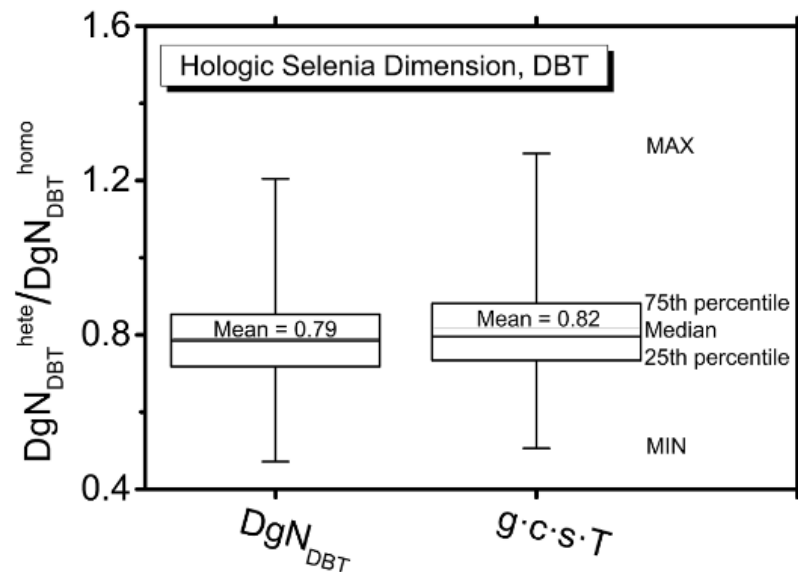
Patient-derived compressed digital breast phantoms



Sarno A et al. "Dataset of patient-derived digital breast phantoms for in silico studies in breast computed tomography, digital breast tomosynthesis, and digital mammography." Medical Physics 48.5 (2021): 2682-2693; Dataset available on zenodo.org, <https://doi.org/10.5281/zenodo.4529852> and <https://doi.org/10.5281/zenodo.4515360>

Sarno A et al. "Comparisons of glandular breast dose between digital mammography, tomosynthesis and breast CT based on anthropomorphic patient-derived breast phantoms." Physica Medica 97 (2022): 50-58.

Is a new paradigm necessary in x-ray breast imaging dosimetry?

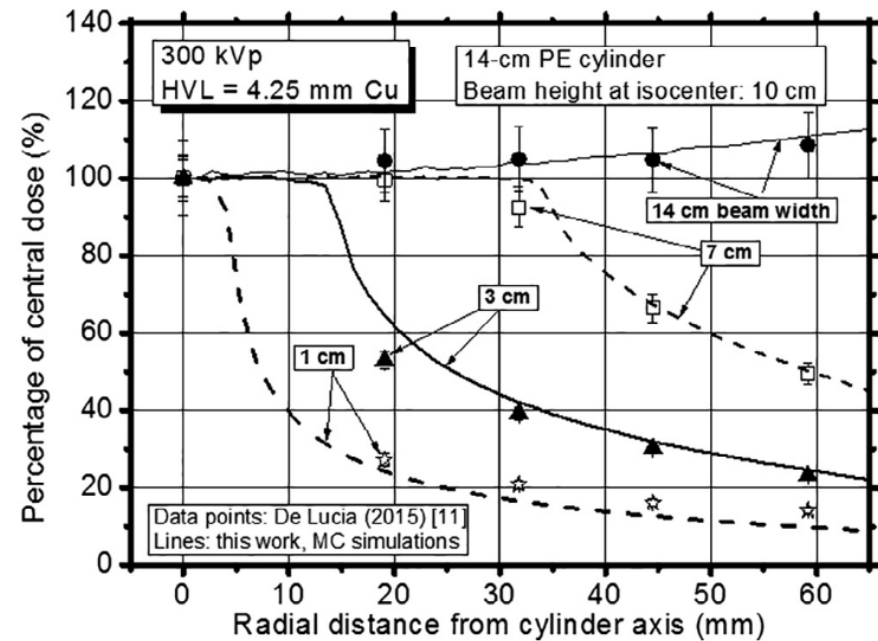
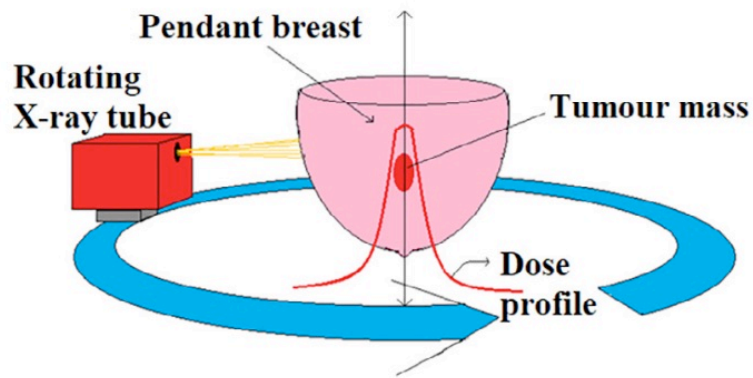


Sarno A et al. "Homogeneous vs. patient specific breast models for Monte Carlo evaluation of mean glandular dose in mammography." *Physica Medica* 51 (2018): 56-63.

Sarno A et al. "Comparisons of glandular breast dose between digital mammography, tomosynthesis and breast CT based on anthropomorphic patient-derived breast phantoms." *Physica Medica* 97 (2022): 50-58

Sarno A et al. "Monte Carlo evaluation of glandular dose in cone-beam X-ray computed tomography dedicated to the breast: Homogeneous and heterogeneous breast models." *Physica Medica* 51 (2018): 99-107.

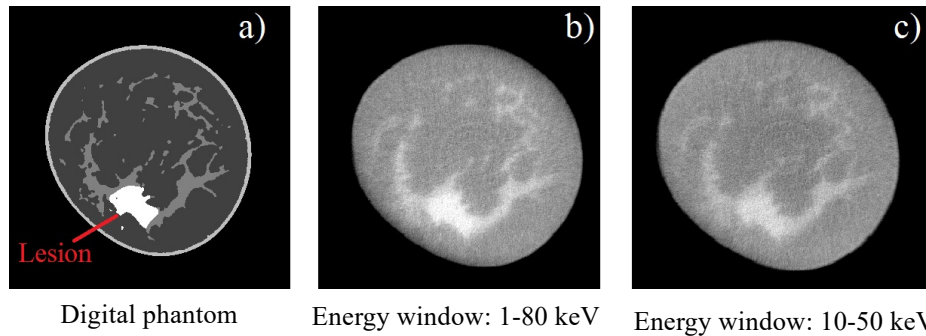
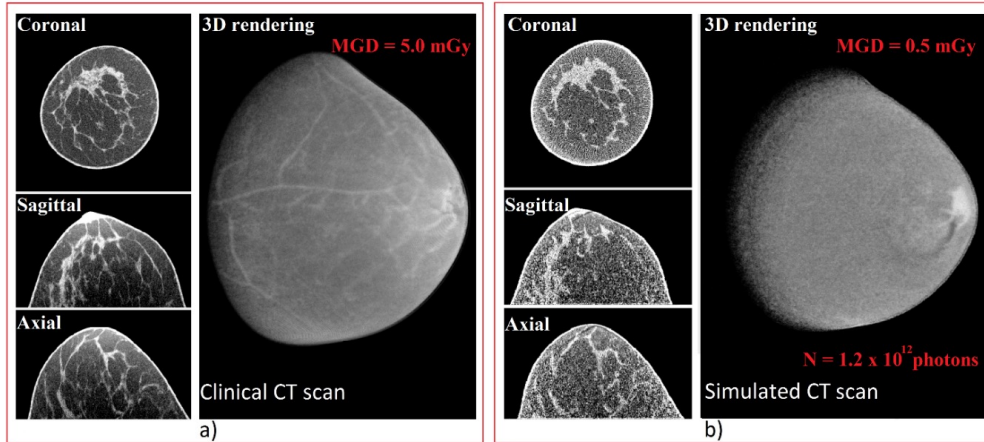
Kilovoltage rotational breast radiotherapy: innovative approach at low photon energy



MC simulation and experimental validation at 300 kV of a technique initially proposed by J. Boone 2012

Buonanno F. et al. "Rotational radiotherapy of breast cancer with polyenergetic kilovoltage X-ray beams: An experimental and Monte Carlo phantom study." *Phys Med* 62 (2019): 63-72.

Virtual clinical trials in x-ray breast imaging: the AGATA project



di Franco F et al (2020). GEANT4 Monte Carlo simulations for virtual clinical trials in breast X-ray imaging: Proof of concept. *Physica Medica*, 74, 133-142.

Sarno A et al. "Advanced Monte Carlo application for in-silico clinical trials in X-ray breast imaging." *IWBI2020*. Vol. 11513. SPIE, 2020.

*Further details in the presentation that will be taken by A. Sarno "Noise in accelerated in-silico x-ray breast images: impact on the breast anatomy and the detector", Monday, Sess II

New models for dosimetry in CT: 3D optical scanning for personalized dose estimates before the CT scan

Male adult



Female adult



Relative discrepancies between standard and customized phantoms

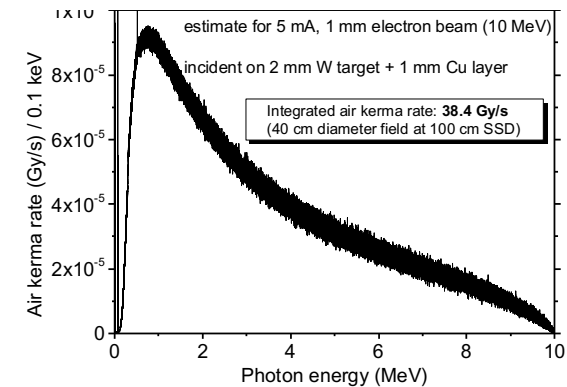
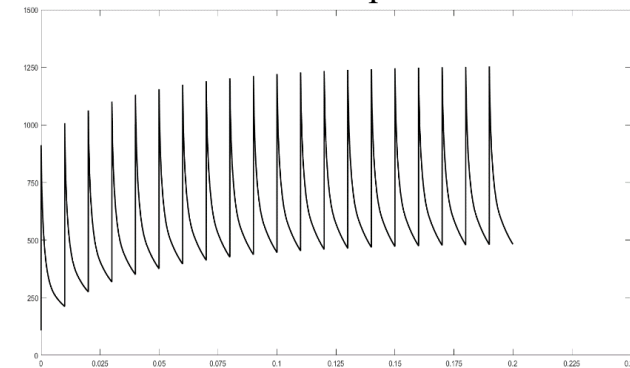
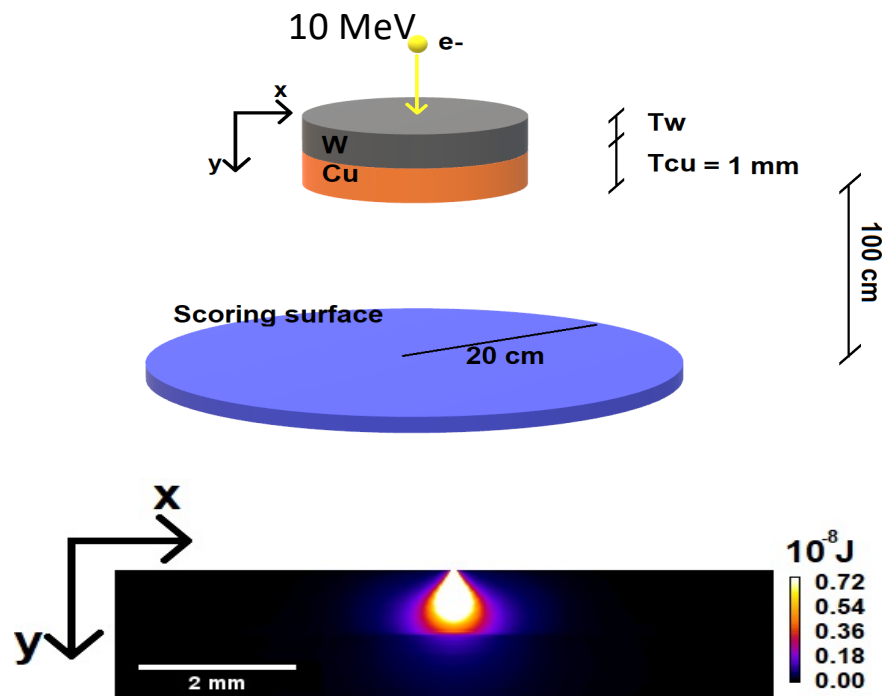
Tube spectrum	Brain	Eyeballs dose	Lens dose	Pituitary gland dose
80 kV	+0.8	-7.4	-10.2	+4.9
100 kV	-2.7	-9.2	-13.1	-0.7
120 kV	-4.5	-10.0	-12.2	-4.1
135 kV	-5.1	-9.9	-13.7	-4.9

Tube spectrum	Brain	Eyeballs dose	Lens dose	Pituitary gland dose
80 kV	+17.9	+8.9	+4.7	+20.4
100 kV	+36.3	+30.8	+28.2	+38.0
120 kV	+22.2	+17.6	+14.9	+23.3
135 kV	+24.4	+16.8	+3.0	+6.6

*Further details in the presentation that will be taken by F.S. Maddaloni "Geant4 Monte Carlo simulations for size specific organ dose estimates in CT based on patient silhouette and voxelized phantoms", Monday, Sess II

X-ray flash radiotherapy: simulation of beam production for the new BriXSino high brilliance source

Temperature over the time: Max target temperature (1200 °C)
for 10^9 electrons/pulse at 100 Hz



*Further details in the presentation “Monte Carlo optimization of the target configuration for bremsstrahlung x-ray production in flash radiotherapy”, Tuesday, Sess IV



IV Geant4 International User Conference 2022, 24–26 October 2022, Napoli (Italy)

Welcome in Napoli and have an amazing conference!!!



sarno@na.infn.it